Int. J. Electrochem. Sci., 17 **(2022)** Article Number: 221255, doi: 10.20964/2022.12.63

International Journal of
ELECTROCHEMICAL
SCIENCE
www.electrochemsci.org

Corrosion Control of Carbon Steel in Acidic Media by Nonionic Surfactant Compounds Derived from 1,3,4-Oxadiazole and 1,3,4-Thiadiazole

M. Abdallah[1,2,*], *Tasnem Al-Habal*[1], *Refat El-Sayed*[3], *M.I.Awad*[1], *R.S. Abdel Hameed*[4,5],

[1] Chem. Depart. Faculty of Appl. Sci., Umm Al-Qura University, Makkah, Saudi Arabia.
[2] Chem. Depart. Faculty of Sci., Benha University, Benha, Egypt.
[3] Chem. Depart. Univ. College in Al-Jamoum, Umm Al-Qura Univ., Makkah, Saudi Arabia
[4] Chem. Depart. Faculty of Sci., Al-Azhar Univ., 11884 Egypt.
[5] Basic Sci., Depart. Prepar. Year, Hail Univ., Hail, 1560 Saudi Arabia
[*]E-mail: metwally555@yahoo.com

Received: 27 October 2022 / *Accepted:* 28 November 2022 / *Published:* 27 December 2022

Two nonionic surfactants molecules (NSM) compounds derived from 1,3,4- oxadiazole and 1,3,4-thiadiazol were synthesized and identified by FTIR and ^{1}HNMR. The synthetic molecules were tested as corrosion inhibitor for carbon steel (CSt) in 1.0M HCl solutions utilizing chemical and electrochemical methods. Inhibition efficacy(%IE) rises with rising concentration of NSM. It is reached 86.76% and 89.78 % for NSM compounds I and II, respectively, The %IE values minimized at elevated temperature demonstrating the physical adsorption of NSM compounds on the CSt surface. Potentiodynamic polarization proved the NSM are mixed inhibitors. The inhibitory strength of these molecules was interpreted on the fundamental of its adsorption on the CSt surface. The adsorption is subjected to Langmuir isotherm. There is a good agreement between the values of %IE and the surface properties values for the interpretation of the inhibitory activity of NIS compounds

Keywords: Nonionic surfactants, Carbon steel, Inhibitor, Impedance, Adsorption

1. INTRODUCTION

Carbon steel (CSt) is utilized in many important technological industries, whether in factories or the construction of buildings, bridges, petroleum pipelines and other industries. Sulfuric acid is utilized in several industries during pickling and cleaning, of CSt. Unfortunately, sulfuric acid causes corrosion of CSt, so scientists have turned to solving this problem by using many ways, one of the most notable is the application of corrosion inhibitors [1,2]. Organic molecules that have hetero atoms and/or aromatic rings in their chemical structure are applied as an effective inhibitor for steel in acidic solutions [3-14].

Typically, these molecules are controlling the dissolution of steel by adsorbing it on its surface by formation chemisorbed of physiosorbed layer on the steel surface [15]. The adsorption creates a barrier that insulates the steel interface from the acidic solution and thus reduces the rate of corrosion. However, adsorption relied on the type and surface condition of the metal, the nature of the corrosive solution, and the chemical structure of the inhibitor [16].

Most of the organic compounds diminishes the corrosion rate of steel in an acidic environment and give a good inhibition efficacy, but unfortunately, they are harmful to the environment and human health as well as their cost is high. Therefore, researchers turned to using some surfactant molecules to control the corrosion of steel in acidic solution [17-25]. Surfactants are organic molecules with unparalleled properties owing to their amphipathic molecule. They have many advantages to be applied as corrosion inhibitors such as, easily adsorbed on the metal surface which led to give high inhibition efficacy, its economic cost is profitable, environmentally friendly and harmless to human health and easy to prepare [26]. Nonionic surfactants were applied as inhibitors for corrosion of steel in acidic solutions and gives a good inhibitory efficacy [27- 32].

Strategic objective of this study is the synthesis of two compounds of non-ionic surfactants molecules (NSM) derived from1,3,4- oxadiazole and 1,3,4- thiadiazol. These compounds were confirmed using some of analytical data and tested as inhibitors for CSt in a 1.0M HCl solution. Weight loss (WL), potentiodynamic polarization (PDP)and electrochemical impedance spectroscopy (EIS) techniques were applied to measure the corrosion parameters and the inhibition effectiveness of the two compounds. The impact of temperature was also investigated and the thermodynamic activation functions were evaluated. The relationship between inhibitory activity and surface variables was also investigated.

2. EXPERIMENTAL

2.1. Chemical and electrochemical techniques

Corrosion techniques were done on carbon steel (CSt) which have the composition (weight percent %): 0.091 carbon , 1.27 manganese, 0.002 sulfur, 0.008 phosphor, 0.202 silicon, 0.035 aluminum , 0.046 vanadium, 0205 nickel, 0.011 chromium and the balance is iron. All chemicals used were purchased from Sigma- Aldrich. The corrosive HCl solution and the examined NSM were prepared using twice distilled water. For weight loss (WL) techniques a coupon with dimensions 1 ×1.85× 0.22 cm^3 are used. For potentiodynamic polarization (PDP) and electrochemical impedance spectroscopic (EIS) methods. A CSt rod immersed in epoxy with an uncovered area of 0.36 cm^2 was used. Firstly, the CSt coupons or rods were sanded with various emery papers until to 2000 degrees, after which they are cleaned with twice distilled water and acetone and then dried between two filter papers. All WL measurements were performed in a temperature-controlled routine. The methods of WL as mentioned earlier [33]. PDP measurements were done using a PS remote potentiostat with PS6 software to determine the corrosion functions the electrolytic cell. This cell contains three electrodes: a Pt counter electrode, calomel electrode and CSt electrode. The sweep rate was adjusted at sweep rate equal to 2.0

mV/sec. EIS measurements were done in a frequency range of 100 kHz to 0.1 Hz with an amplitude of 4.0 mV by utilizing a computer- controlled potentiostate (Auto Lab 30, Metrohm).

2.2. Synthesis of nonionic molecules derived from oxadiazole 2 and thiadiazol 3

The Gallen Kamp device was used to determine the melting points. The FTIR 8300 Shimadzu spectrophotometer for observing the infrared spectra. The nuclear magnetic resonance (NMR) spectra utilizing a Bruker AC300 spectrometer [300 MHz for ^{1}H and 75 MHz for ^{13}C], using solvent the deuterochloroform. The microanalysis was performed using element analyzers (EA3000 EURO VECTOR).

2.3. Synthesis of the targets (2 and 3)

3.2.1. Synthesis of N-phenyl-5-undecyl-1,3,4-oxadiazol-2-amine (2)

A mixture of hydrazide 1 (2.14g, 0.01 mol), and phenyl isothiocyanate (1.35g, 0.01 mol) in dimethylformamide (20 mL), was heated under reflux for 8 hrs, the reaction was cooled-down and evaporated the solvent under reduced pressure. The solid product obtained was crystallized.

3.2.2. Synthesis of 5-undecyl-1,3,4-thiadiazole-2(3H)-thione (3)

A finely powdered KOH (1.12g, 0.02 mol) in ethanol (30 mL) and hydrazide **1** (2.14g, 0.01 mol) was added, then (0.76 g, 0.01 mol) of carbon disulfide was slowly added over a period of 10 min. Stirring of the reaction mixture was sustained for additional 1 hr, after complete addition. The reaction mixture was heated under reflux on a steam bath for 12 hrs, then concentrated the solution, cooled and acidified with diluted H_2SO_4. The solid mass that precipitated was filtered, washed with ethanol, dried and recrystallized.

2.4. Synthesis of nonionic molecules (I and II) from the obtained targets (2, 3).

Addition of propylene oxide (5 moles) to some the synthesized compounds (0.1 mol) in each case, using KOH as catalyst [34]. The quantity of propylene oxide which allowed to react and the average degree of propoxylation were measured through the increment in mass of the reaction mixture (increasing of weight of mixture after addition of propylene oxide is the average amount of propoxylation). Normally, addition of propylene oxide gave mixture of propoxylated products and their structures were confirmed on the basis of IR and ^{1}H NMR spectra.

2.5. Estimation of the surface characteristics of targets (I, II)

DuNouy tensiometer (Kruss K_6) was applied to measurements of surface and interfacial tension [35], the critical micelle concentration *(CMC)* [36,37] and Maximum surface excess Γ_{max} (using Gibbs equation [$\Gamma_{max} = -1/ RT[d\gamma/d\log c]$) [38] at 25°C with for various concentrations of the nonionic targets.

3. RESULTS AND DISCUSSION

3.1. Synthesis of oxadiazole 2 and thiadiazole 3 derivatives

The reactivity of hydrazide **1** [prepared by treatment of ethyl dodecanoate with hydrazine hydrate] towards different nucleophiles was studied with respect to the synthesis of highly substituted oxadiazole and thiadiazole targets. Thus, hydrazide **1** with phenyl isothiocyanate was refluxed in dimethylformamide for 8 hr, afford oxadiazole target **2**. On the other hand, heating of hydrazide **1** with carbon disulfide, potassium hydroxide affords thiadiazole target **3**. (**Scheme 1**). The physical properties and spectral data for the confirmation of the structure was summarized in **Tables (1**,**2)**.

3.2. Synthesis of nonionic targets (I and II).

Nonionic heterocyclic molecules are efficiency class having good surface properties owing to the struggle between the alliance of hydrophilic and hydrophobic structure and their biological activity. Thus, hydroxylation of the obtained targets **(2,3)** with propylene oxide (5 moles) gave 2,5,8,11-tetramethyl-1-(phenyl(5-undecyl-1,3,4-oxadiazol-2-yl)amino)-3,6,9,12-tetraoxapentadecan-14-ol **(I),** and 3-(14-hydroxy-2,5,8,11-tetramethyl-3,6,9,12-tetraoxapentadecyl)-5-undecyl-1,3,4-thiadiazole-2(3*H*)-thione **(II)**, respectively.

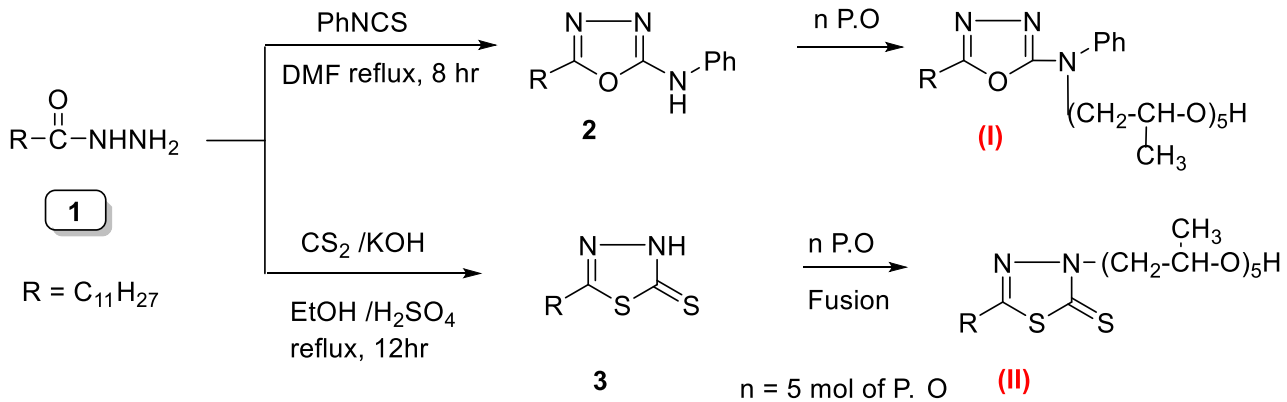

Scheme 1: Synthesis of oxadiazole and thiadiazole derivatives

Target	Chemical structure	IUPAC Name
I	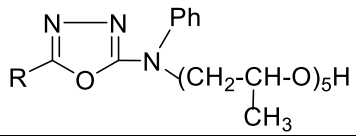	2,5,8,11-tetramethyl-1-(phenyl(5-undecyl-1,3,4-oxadiazol-2-yl)amino)-3,6,9,12-tetraoxapentadecan-14-ol
II	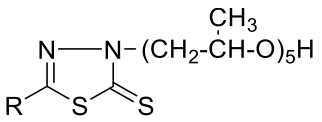	3-(14-hydroxy-2,5,8,11-tetramethyl-3,6,9,12-tetraoxapentadecyl)-5-undecyl-1,3,4-thiadiazole-2(3*H*)-thione

Table 1. Physical data of the targets **(2 and 3)**

No.	M.F	M.Wt	m.p. °C	Yield (%) Weight (g)	Color Solvent	Analysis data calc. / Found %			
						C	H	N	S
2	$C_{19}H_{29}N_3O$	315.45	96-98	(65) 1.39	Yellow EtOH/DMF	72.34 72.61	9.27 9.57	13.32 13.11	
3	$C_{13}H_{24}N_2S_2$	272.47	125-127	(71) 1.51	Yellow Ethanol	57.30 57.02	8.88 8.56	10.28 10.43	23.54 23.79

Table 2. Spectroscopic data for the synthesized targets.

No.	IR	^{1}H NMR
2	1597, 1618 (C=N), 2848, 2950 (CH aliph), 3091 (CH arom), and 3221 (NH)	0.89 (3H, t, CH_3), 1.26-1.36 (20H, m, CH_2 alkyl), 7.38-7.47 (5H, m, ArH), and 8.00 (2H, s, NH).
3	1603 (C=N), 2635 (CS), 2848, 2919, (CH aliph) and 3225 (NH).	0.89 (3H, t, CH_3), 1.24 -1.39 (20H, m, CH_2 alkyl), and 10.75 (s, 1H, NH).
I	Two bands in region (900-960) and (1100-1170) for (ether likage of polypropoxy chain), and 3200-3400 for (OH).	Multiple signals in region of (3.3–3.8) for the propoxy groups
II	Two bands in region (1100, 1145) and (889-950) for (ether linkage of polypropoxy chain) and 3330-3405 for (OH).	The propoxy groups appear as multiple signals in region of (3.0–3.8).

3.2. PDP measurements

PDP curves of the CSt in 1.0 M HCl solutions and when it involves certain concentrations of surfactants compounds I and II are represented in Fig 1**.**

Obviously from this figure . at the start of polarization. The current density change slowly or remains constant to the anodic or cathodic direction . This is defined transition zone. After this zone, the potential decreases or increases rapidly in case of cathodic or anodic polarization (Tafel plots) [39].With increasing the surfactant compounds concentrations from 100 to 500 ppm, the Tafel lines are shifted to more active(-ve) and noble (+ve)potentials to the free HCl curve. Thus, NSM influences both cathodic H_2 evolution and the anodic reaction of CSt [40].

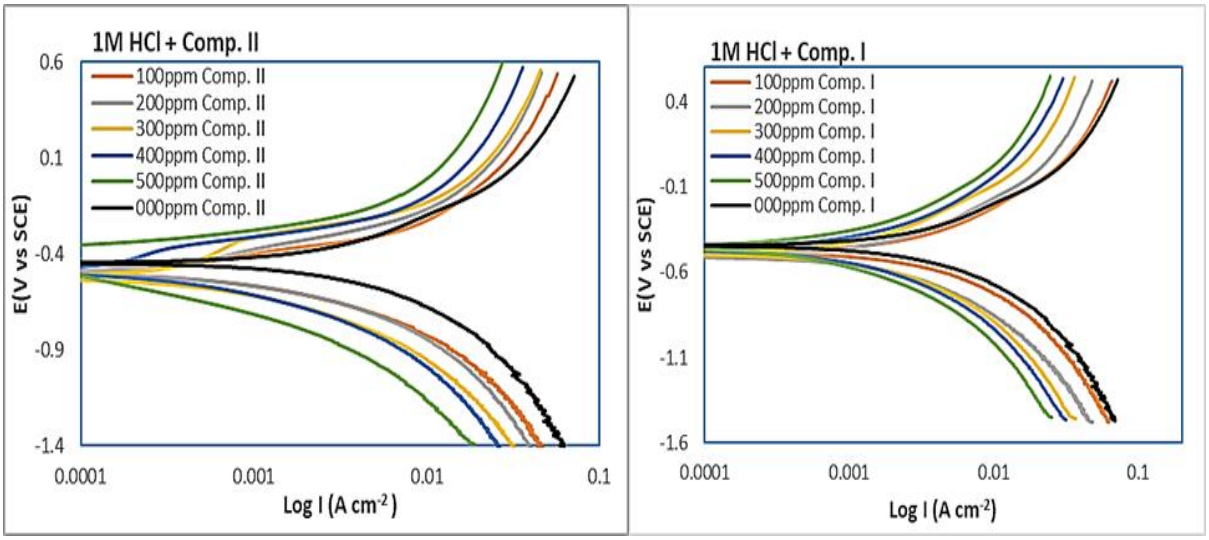

Figure 1. PDP curves for CSt in 1.0 M HCl and when it includes certain concentrations of (A) comp. I and (B) comp. II at 300K

Certain corrosion functions have been determined from Fig.1, e.g., anodic (β_a), cathodic (β_c), corrosion current density (I_{corr}) which is computed from the extrapolation of the anodic and cathodic Tafel lines with corrosion potential (E_{corr}), and inhibition efficacy(%IE) These parameters are collected in Table 3. The values of %IE for the two NSM were computed utilizing the next equation

$$\% IE = \left[1 - \frac{I_{add}}{I_{free}}\right] 100 \qquad (1)$$

where, I_{free} and I_{add} are the corrosion current densities in the free1.0 M HCl and when added certain concentrations of the surfactant compounds, respectively.

By examining Table 3, it is clear that the values of β_a and β_c are almost constant, the shift in case of compound I from the free 1.0 M HCl solution being about 7 and 19 mV in case of β_a and β_c , respectively. While the shift in case of compound II from the free 1.0 M HCl solution is about 6 and 18 mV in case of β_a and β_c , respectively. This confirms that the compounds I &II retards the dissolution of CSt and cathodic hydrogen evolution. The change in the values of $E_{corr.}$ is about32 and 36 mV. The shift in the potential are less than 85 mV . From the values of β_a and β_c and the lower shift in $E_{corr.}$ demonstrated that he surfactants compounds I and II are mixed inhibitors. As the concentration of compounds I and II are augment, $I_{corr.}$ values are minimized and the %IE values are rises which demonstrates the inhibitory effect of the two surfactant compounds. At the same concentrations the %IE values for compound II are more than for compound I.

3.3. EIS measurements

Fig. 2 (A&B) illustrates the Nyquist diagram for CSt electrode in 1.0 M HCl solution alone and also with existence of some concentrations of surfactants compounds I and II at 300K. The semicircular behavior are acquired incase in free acid solutions and the existence of various concentrations ranged

from 100 to 500 ppm of compounds I&II demonstrating the dissolution of CSt electrode is principally done by charge transfer process[41].

Table 3. Corrosion parameters acquired from PDP of CSt in 1.0 M HCl containing some concentrations of two NSM.

Medium	Inh. Conc.	$-\beta_c$, mV dec.$^{-1}$	β_a , mVdec^{-1}	$-E_{corr}$ mV, (SCE)	I_{corr} (µA/cm^2)	%IE
Blank	**1.0 M HCl**	898	835	-432	9.59	-
Comp.I	1M HCl + 100ppm	885	828	-469	5.33	44.42
	1M HCl + 200ppm	883	833	-495	4.04	57.87
	1M HCl + 300ppm	882	838	-472	2.81	70.69
	1M HCl + 400ppm	879	842	-467	2.39	75.08
	1M HCl + 500ppm	879	824	-464	1.27	86.76
Comp. II	1M HCl + 100ppm	993	835	-510	4.88	49.11
	1M HCl + 200ppm	990	838	-476	3.13	67.36
	1M HCl + 300ppm	986	835	-460	2.16	77.48
	1M HCl + 400ppm	982	833	-458	1.47	84.67
	1M HCl + 500ppm	980	830	469	0.98	89.78

The diameter of the capacitive loop increases on addition of NSM I and II which confirms the construction of protective film on the CSt curface [42]. The Nyquist plots were done by appropriate the results to a simple equivalent circuit which appear in Fig. 3. which involves the solution resistance (R_s) and the double layer capacitance (C_{dl})which is placed in parallel to the charge transfer resistance(R_{ct})[31,42].

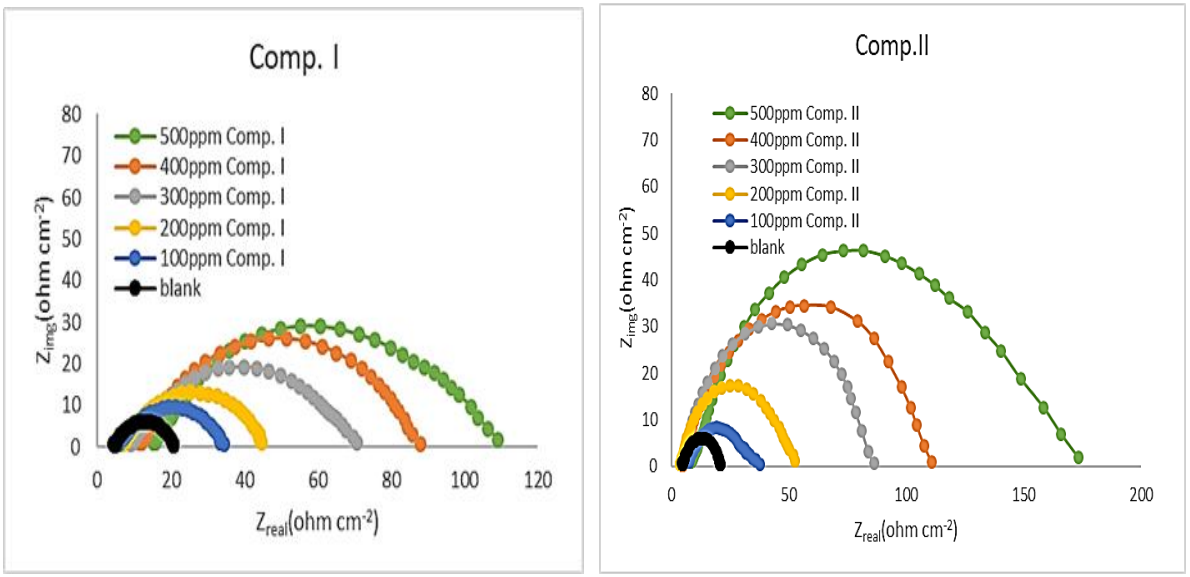

Figure 2. Nyquist plots for CSt in 1.0 M HCl solution and when including some concentrations of (A) comp. I and (B) comp. II at 27ºC

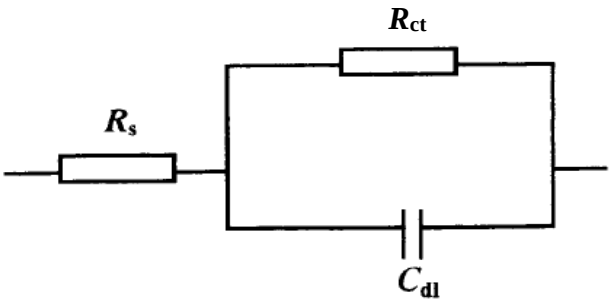

Figure 3. The equivalent circuit model utilized to fit the experimental data.

The parameters are acquired from Nyquist diagram are R_{ct} which is the diameter of the high frequency loop.The C_{dl} values is determined from below relation

$$C_{dl} = \frac{1}{2\pi f_{max} R_{ct}} \quad (2)$$

Where f_{max} is the maximum frequency.

The %IE values from EIS technology were determined by the subsequent relation:

$$\%IE_{(b)} = \left[\frac{(1/R_{ct})_o - (1/R_{ct})}{(1/R_{ct})_o}\right] x100 \quad (3)$$

where,$(R_{ct})_o$ and(R_{ct}) are the values of the charge transfer resistance in the 1.0 M HCl solution and when added certain concentrations of the surfactant compounds, respectively.

Table 4. Corrosion data from EIS method of CSt in 1.0 M HCl alone and when including some concentrations of two NSM

Medium	Inh. Conc.	R_s (Ω cm²)	C_{dl} (μF cm^{-2})	R_{ct} (Ω cm²)	%IE
Blank	**1.0 M HCl**	4.6	13.32	20.6	--
Comp.I	1M HCl + 100ppm	5.6	7.62	35.6	42.13
	1M HCl + 200ppm	7.0	6.84	46.0	55.22
	1M HCl + 300ppm	9.2	4.08	71.0	70.99
	1M HCl + 400ppm	11.6	3.46	88.6	76.75
	1M HCl + 500ppm	15.4	2.14	109.4	81.17
Comp. II	1M HCl + 100ppm	6.6	7.08	37.6	45.21
	1M HCl + 200ppm	3.7	6.13	53.7	61.64
	1M HCl + 300ppm	4.0	3.77	86.0	76.05
	1M HCl + 400ppm	4.4	2.06	111.4	81.51
	1M HCl + 500ppm	8.3	0.97	173.3	88.11

The associated EIS functions such as *R*s, C_{dl}, R_{ct} and % IE are incorporated in Table 4. Clearly from these functions , with rising the concentration of compounds I and II, the C_{dl} values minimized owing to the exchange of the water molecule on the surface of CST by NSM leads to the construction of a oxide film on the surface of CSt and the result is a minimization of the dielectric constant of the steel solution interface. R_{ct} values and %IE rises due to the constructing an adhesive film on the CSt /solution interface. At the same similar concentrations of two compounds, the %IE values for compound II are more than those of compound I.

3.4. Weight loss (WL) methods

3.4.1. Effect of surfactant concentrations

The relation between the WL curves and the inundation time curves of CSt coupons in1.0 M HCl and in the exitance of certain concentrations of NSM I and II are represented in Fig 4(A&B), respectively. Obviously, the WL declines with increasing the inundation time. This demonstrates that the inhibitory activity of compounds I & II towards the dissolution of CSt in 1M HCl solutions. A linear relationship in free HCl and in presence of NSM was acquired in Fig.4 indicating the freed from any insoluble surface layers during corrosion. In this case the NSM are firstly adsorbed on the CSt surface and hence retard the corrosion .

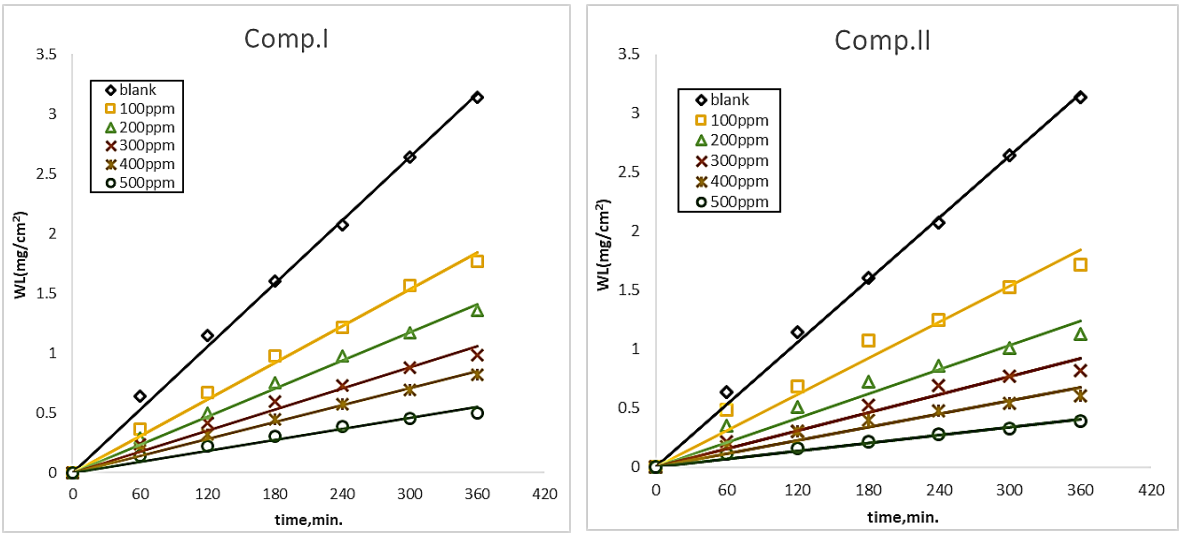

Figure 4. weight loss plots for CSt in 1.0 M HCl solution alone and when containing including some concentrations of (A) comp. I and (B) comp. II at 300 K

The rate of corrosion of CSt($R_{corr.}$) was determined from the next equation [43,44]

$R_{corr.} = \Delta WL/St$ (4)

Where, ΔWL is the difference in the WL of CSt before and after inundation in the investigating surfactant solutions, S is the surface area in cm^2 and t is the inundation time in hours.

Table 5. Corrosion parameters acquired from WL measurements

Inh.	Inh. Conc. (ppm)	ΔWL(mg)	R_{corr} x10^{-3} (mg cm^{-2} min^{-1})	Θ	IE %
-	1M HCl	50.2	8.715	-	-
Comp. I	1M HCl + 100ppm	28.3	4.913	0.436	43.63
	1M HCl + 200ppm	21.7	3.767	0.568	56.77
	1M HCl + 300ppm	15.7	2.726	0.687	68.73
	1M HCl + 400ppm	13.1	2.274	0.739	73.90
	1M HCl + 500ppm	8.0	1.389	0.841	84.06
Comp. II	1M HCl + 100ppm	27.5	4.774	0.452	45.22
	1M HCl + 200ppm	18.0	3.125	0.641	64.14
	1M HCl + 300ppm	13.1	2.273	0.739	73.92
	1M HCl + 400ppm	9.7	1.684	0.807	80.68
	1M HCl + 500ppm	6.2	1.075	0.877	87.67

The inhibition efficacy (% IE_{WL}) and the surface coverage (θ) were determined bt application of the next equations:

$$\text{IE \%} = \left[1 - \frac{R_{add}}{R_{free}}\right] 100 \quad (5)$$

$$\theta = \left[1 - \frac{R_{add}}{R_{free}}\right] \quad (6)$$

where, R_{free} and R_{add} are the rate of corrosion of Al in free HCl solution and when it contains some concentricity of surfactant compounds respectively.

The determined functions from WL measurements, such as R_{corr}, θ and %IE and θ are listed in Table 5. Clearly from Table 1. Wih increasing concentration of surfactant compounds I &II. The R_{corr} values are reduced while the values of %IE and θ are increased . This suggested that the inhibition impact of NSM towards the corrosion of CSt in 1.0M HCl solution. %IE of compound is more than compound I

3.4.2. Influence of high temperature

The influence of high temperature from 295 to 325 K on the dissolution of CSt in 1.0 M HCl solution and when including 500 ppm of compound I and II was investigated utilizing weight loss method. Analogous curves were acquired in Figure 4 but not appear. The R_{corr} and IE% values were determined and recorded in Table 6. From the data in this table, we find that with increasing the temperature, the loss in weight and the R_{corr} increase and the IE % decreases. This demonstrates that the adsorption of NSM compounds I and II on CSt surface are physical. The high temperature led to desorption of the adsorbed surfactant compounds from the CSt surface.

Table 6. Impact of temperatures on the corrosion functions of CSt in a free 1.0 MH_2SO_4 and when containing 500ppm of compounds I and II.

	Temp.,K	ΔWL(mg)	R_{corr} x10^{-3} (mg cm^{-2} min^{-1})	%IE
1.0MHCl	295	50.2	8.715	-
	305	60.4	10.509	-
	315	69.7	12.128	-
	325	78.6	13.676	-
1.0MHCl+500ppm of comp.I	295	8.0	1.389	84.06
	305	10.8	1.879	82.12
	315	13.8	2.401	80.20
	325	16.2	2.818	79.39
1.0MHCl+500ppm of comp.II	295	6.2	1.075	87.67
	305	8.5	1.479	85.93
	315	11.2	1.948	83.94
	325	13.4	2.332	82.94

Arrehenius equation is applied to determine the activation energy (E_a) of CSt in 1M HCl solution and when contains 500ppm of compounds I and II according to the next equation[45,46]:

$$R_{corr} /A = e^{-Ea/RT} \quad (7)$$

Where, A is Arrhenius constant, R is the gas constant and T is the absolute temperature.

The relation between the log R_{corr}. and 1000/T for CSt in 1M HCl solution and in the occurrence 500ppm of compounds I and II was represented in Fig 5. Straight lines relationship were gained. The E_a values were determined from the slope of straight lines and equal to 12.56 KJ mol^{-1} in 1M HCl and 19.25 and 22.96 KJ mol^{-1} for compounds I, and II, respectively. The E_a values increase in presence of surfactant compounds than in acid free solution indicating the adsorption of compounds I and II on CSt surface forming a barrier for mass and charge transfer.

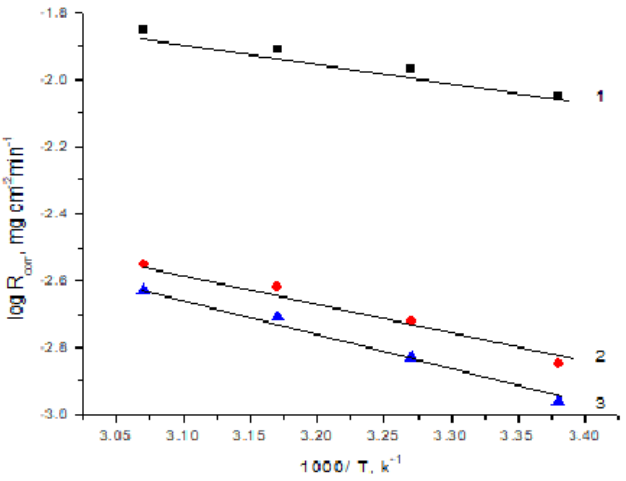

Figure 5. The relationship between log R_{corr} and 1/T for CSt in 1.0M HCl contains 500ppm of compounds I an II . 1) 1M HCl 2) 500ppm comp.I 3) 500ppm comp.II

The enthalpy (ΔH^*) and entropy(ΔS^*)of activation for CSt in 1M HCl solution only and in existence of surfactant compounds were determined by transition state relation [45,46]:

$$R_{corr.}/T = R/Nh\ e^{(\Delta S^*/R - \Delta H^*/R .1/T)} \quad (8)$$

where, h and N are is Planck's and N is Avogadro's number constant .

The relationship between the logarithmic of $R_{corr.}/T$ and 1000/T for CSt in free 1M HCl solution and in the existence of 500ppm of compounds I and II was displayed in Fig 6. Straight lines were gained with a slope of (-ΔH*/2.303 R) and an intercept [log (R/Nh -ΔS^o /2.303R)].

The ΔH* values was acquired from the slope of straight lines and equal to 11.48 KJ mol^{-1} in 1M HCl and equal 21.06 and 22.12 KJ mol^{-1} for compounds I, and II. The positive signs of ΔH* demonstrate that the adsorption process of two NSM on the CSt surface is endothermic nature [47].

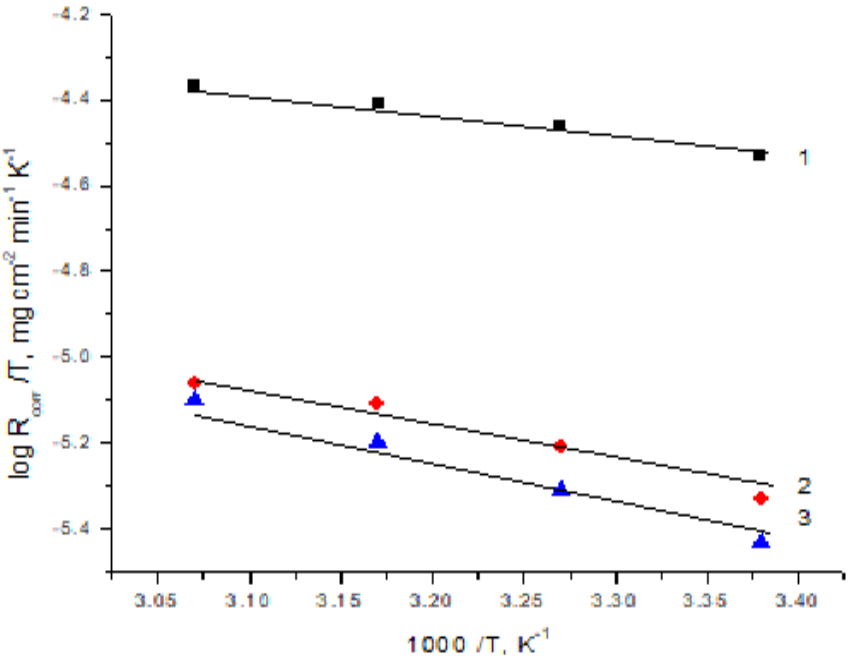

Figure 6. The relation between log $R_{corr.}$ /T and 1/T for CSt in 1.0M HCl contains 500ppm of compounds I an II. 1) 1M HCl 2) 1M HCl+500ppm comp.I 3) 1M HCl+500ppm comp.II

The values of ΔS^* was determined from the intercept of a straight line and equal to - 165.22 J mol^{-1} k^{-1} in 1.0MHCl solutions and -213.24 and 235.24 J mol^{-1} k^{-1} for compounds I and II respectively. The negative signs of ΔS* confirm that the activation complex formation is the rate determining step represents an binding rather than dissociation [48].

3.5. Investigation of surface properties

The activity of the nonionic targets I and II based on the hydrophobic and hydrophilic part was determined and listed **Table 7**.

3.5.1. Surface tension (ST) and interfacial tension (IFT)

The change in nature of a surface or interface between two phases is called surface activity. Where, the adsorption of any substance with the surface of liquid causes a decrease in surface tension of the liquid. The changes in the nature of the interfaces shows high inclination towards adsorption in air and water interface, which a measure of activity of the surface. The results indicated that the targets **I and II** have effective to minimize the surface and interfacial tension values as reflected in **Table 7**.

3.5.2. Critical micelle concentration (CMC)

CMC measure the efficacy of targets, and determine the amount of target needed to reach maximum reduction of surface tension indicates. Within a given series of structurally related the surfactants leading to lower surfactants are expected to reduce the CMC value. As outlined in **Table 7**, the compound II had decreased CMC value which attributed to the lower solubility of nonionic molecules.

3.5.3. Maximum surface excess (Γ_{max})

The amount of target adsorption on a liquid surface is expressed in terms of its surface excess concentration (Γ_{max}). The extra surface varies with molecular structure, which showing more surface area per molecule with a long chain indicating that the targets are less tightly packed at the air/water interface of flexible and long chain surfactants. The outcomes indicate that the result of increasing Γ_{max} causes crowding of the interface resulting in lower amine values as the **Table 7**.

Table 7. Surface properties of the NSM (I and II)

Compounds	ST (dyne/cm) 0.1 m/l	IFT (dyne/cm) 0.1 m/l	CMC mmol/L	Γ_{max} (mol/m^2)
I	44	19	1.70	3.58×10^{-6}
II	40	12.5	1.44	3.83×10^{-6}

3.6. Adsorption isotherm and Mechanism of inhibition

Surfactants compounds I and II minimize the corrosion of CSt in 1MHCl solution by adsorbing them on their surface. The adsorption occurs by replacing a water molecule adsorbed on the CSt surface $(H_2O)_{ads.}$ by surfactant molecule adsorbed on the CSt surface $(Surf.)_{ads}$. Adsorption based on the chemical composition of two surfactant compounds I and II. Concentration of the acid and surfactant concentration, the occurence of active centers to facilitate the adsorption process. Adsorption gives an understanding of the interaction between the adsorbent molecules themselves as well as their interaction with the CSt surface.

The surface coverage (θ) for certain concentrations of compounds I and II were computed from the weight loss experiment and inserted in various isotherms to choose the preferable isotherm. We found that the best fit was acquired with Freundlish isotherm owing to the subsequent equation[49,50]:

$$\log \theta = \log K_{ads.} + n \log C \quad (9)$$

Where, K_{ads} and C are the equilibrium constant of adsorption operation and surfactant concentration, respectively. The Freundlich plots (log θ vs. log C) for the adsorption of two NSM I and II on the CSt surface is displayed in Figure 7. A straight lines were acquired proving the adsorption process obeyed Langmuir isotherms.This elucidate that the absence of the interaction between the two NSM and CSt surface.

From the intercept of this Fig, we can determine the values of K_{ads}. The values of $K_{ads.}$ are equal to(436 and 398) $\times 10^{-3}$ for compounds I and II ,respectively. These values demonstrates the vigorous adsorption of compounds I and II on the CSt surface. The values of free energy of adsorption ($\Delta G°_{ads.}$) are determined from the values of K_{ads}. due to the next equation:

$$K = e^{(-\Delta G°ads/RT)} / 55.5 \quad (10)$$

Where, the value 55.5 is the concentration of water in mol/ l. The values of $\Delta G°_{ads.}$ are equal to -78.14 and -75.91 kJ mol^{-1} for compounds I and II respectively. Negative marks of $\Delta G°_{ads.}$ demonstrates that the adsorption of two NSM on the surface of CSt are spontaneous.

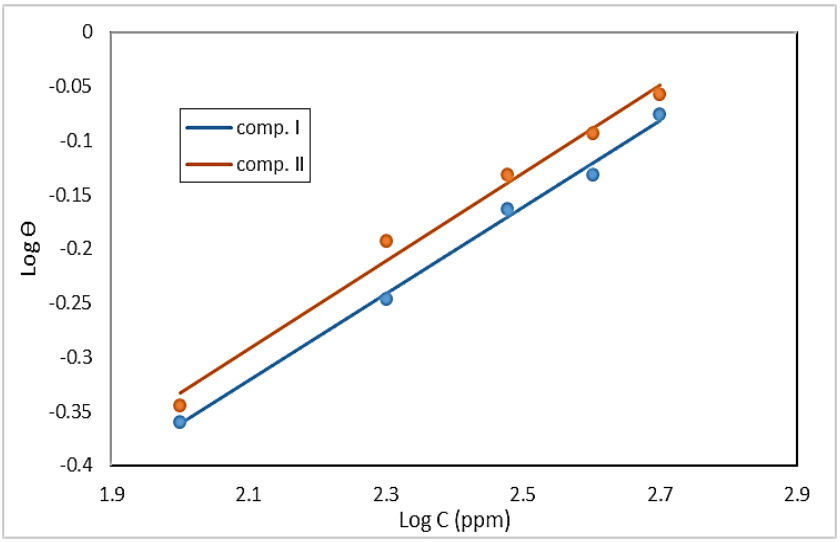

Figure 7. The relation between logarithm of log θ and logarithm of surfactant concentration (log C).

The corrosion parameters of CSt in 1M HCl solution in exitance of NSM was investigated using chemical (WL) electrochemical (PDP&EIS) methods and surface parameters confirm the inhibition of NSM molecules. The %IE of NSM is due to its capability to bind to each other at interfaces and in solution to aggregate to form micelles [51].The accumulation of NSM can be measured by

minimizing the values of ST ,IFT ,CMC and increasing the values of Γ_{max}. These led to increase of the adhesive force between the surface of CSt and NSM and thus an increase the building of an adhesive layer on the surface.

The inhibitory force of NSM on the surface of Cst is due to its adsorption by construction an adsorbent film on its surface.

NSM with a long hydrocarbon chain is adsorbed on the surface of CSt through the hydrophilic portion, which includes oxygen, nitrogen or sulphur atoms. On the other hand, hydrocarbon chains tend to be wrap around in water to reduce the contact area between themselves and water molecule [52].Adsorption of NSM to the surface of the CSt is performed by a propylene oxide unit while the hydrocarbon fractions protrude like a brush into the solution [53]. The %IE of the examined NSM increases with increasing their concentration and the % IE of compound II is more efficient than compound I. This due to the exitance two sulfur atoms facilities the formation of more coordination bonds than compound I which increase the adsorbed layer on the CSt surface and consequently increase the inhibitory efficacy.

4. CONCLUSIONS

1. Synthetics NMS act as an efficient corrosion inhibitor for corrosion of CSt 1.0 M HCl solution.
2. NMS synthesized and identified by FTIR and ^{1}HNMR
3. The inhibition efficiency increases with increasing NMS concentration and lowering temperature
4. The inhibition was explicated according to the potent adsorption of NMS on CSt surface
5. The adsorption is obeyed to Langmuir isotherm.
6. NMS act as mixed inhibitor.
7. The values of corrosion parameters are coincided with surface properties.

References

1. K.S. Jacob and G. Parameswaran, *Corros.Sci.,*52 (2010) 224.
2. M. Abdallah, Basim H. Asghar, I. Zaafarany, A. S. Fouda, *Int. J. Electrochem Sci*., 7 (2012)282.
3. S. Issadi, T. Douadi, A. Zouaoui, S. Chafee, M.A. Khan and G. Bout, *Corros.Sci.,* 53(2011)1484.
4. Ahmed El Defrawy, M. Abdallah, Jabir Al-Fahemi, *J.Mol. Liq.,*288 (2019) 110994.
5. Reda S. Abdel Hameed, A. H. Al-Bagawi, Hassan A. Shehata, Ahmed H. Shamroukh, M. Abdallah, *J. Bio- and Tribo-Corrosio*n **,** 51 (2020)1.
6. M. Abdallah, H.M. Altass, Arej S Al-Gorair, Jabir H. Al-Fahmi, K.A. Soliman, *J. Mol. Liq., 323* (2021) 115036.
7. M. Abdallah, K.A. Soliman, Mubarak Alshareef, Arej S Al-Gorair, H. Hawsawi, Hatem M. Altass Salih S. Al-Junaid , M.S. Mattawa , *RSC Adv.,* 12(2022)20122.
8. R.S. Abdel Hameed, M.T. Qureshi, M. Abdallah, *Int. J. Corros. Scale Inhibit.,* 10 (1) (2021)68.
9. M. Abdallah, M. Alfakeer, H.M. Altass, Ahmed. M. Alharbi, Ismail Althagafi, N.F. Hasan, E.M. Mabrouk,*Egypt. J Petr.,* 28 (2019)393.
10. Z. Hajiahmadi, Z. Taranga, *J.Mol.Liq*., 284 (2019) 225.

11. M. Abdallah, Kamal A. Soliman, Rami Alfattani, Arej S Al-Gorair, A. Fawzy, Mahmoud A. A. Ibrahim, *Int. J . Hydrogen Energy,* 47 (2022) 12782.
12. M. Abdallah, A.M. El- Dafrawy,M. Sobhi, ,A.H.M. Elwahy, M. R. Shaaban, *Int. J. Electrochem Sci.,* 9(2014) 2186.
13. Arej S Al-Gorair, M. Abdallah *Int. J. Electrochem. Sci.,* 16 (2021) 210771.
14. Z. Haji Ahmadi, Z. Taranga, *J. Mol. Liq*., 284(2019) 225.
15. A. A. Olajire, *J. Mol. Liq.*, 248 (2017) 775.
16. H. Tian, W. Li, B. Hou, D. Wang, *Corros. Sci.,* 117 (2017)43.
17. M. Abdallah, M.A. Hegazy, H. Ahmed, B.A.AL Jahdaly, H. Hawsawi, M. Murad, F. Benham, I. Warad, A. Zarrouk , *RSC Adv.,* 12 (2022) 17050.
18. A. Fawzy, M. Abdallah, I. A. Zaafarany, S. A. Ahmed, I. I. Althagafi, *J.Mol.Liq*., 265 (2018) 276.
19. A. Fawzy, M. Abdallah, M. Alfakeer, H. M. Ali., *Int. J. Electrochem. Sci.,* 14 (2019) 2063.
20. R. Mehdaoui, A. Khelifa, A. Khadraoui, O. Aaboubi, A. Hadj Ziane, F. Bentiss, A. Zarrouk, *Res. Chem. Interm.,* 42 (2016), 5509.
21. Wagdy I. El-Dougdoug, Arej S. Al-Gorair , Asmaa Abou Elsaoud, Hana Hawsawi, Ahmed Elaraby, El Sayed Mabrouk, Metwally Abdallah, *Green Chem. Lett. Rev*., 15 (2022)796.
22. A. Fawzy, I. A. Zaafarany, H. M. Ali, M. Abdallah, *Int. J. Electrochem Sci*., 13(2018) 4575.
23. M. Abdallah, M.A. Hegazy, M. Alfakeer, H. Ahmed, *Green Chem. Lett. Rev*., 11(2018) 457.
24. M.A. Hegazy, A.S. El-Tabei, A. H. Bedear, M.A Sadeq, *Corros. Sci*., 54(2012) 219.
25. A. Fawzy, M. Abdallah, M. Alfakeer, H. M. Ali., *Int. J. Electrochem. Sci.,* 14 (2019)2063.
26. M.A. Hegazy, M.F. Zaky, *Corros. Sci.,* 52(2010) 1333.
27. M. Abdallah, H.M. Altass, R. El-Sayed, Arej S. Al Gorair, B.A.AL Jahdaly M. Sobhi, *Prot. Met. Phys. Chem. Surf*., 57(2021) 811.
28. M. Abdallah, R. El-Sayed, A. Mashaei, M. Alfakeer, *Prot. Met. Phys. Chem. Surf*., 57(2021) 389
29. M. Abdallah, M. Alfakeer, Arej S Al-Gorair, A. Al Bahir, M. Sobhi, Int. *J. Electrochem. Sci.,* 16 (2021) 210622.
30. M. Abdallah, R. El-Sayed, A. Mashaba, M. Alfakeer, *Prot. Met. Phys. Chem. Surf*., 57 (2021) 389.
31. M. Sobhi, R. El-Sayed, M. Abdallah, *J. Surf. Deterge.*, 16(2013) 937.
32. Metwally Abdallah, Nizar El Guesmi, Arej S. Al-Gorair, Refit El-Sayed, Aseel Mashaba, Mohamed Sobhi, *Green Chem. Lett. Rev.*, 14 (2021) 381.
33. P.B. Mathur, T. Vasudevan, *Corrosion,* 38(1982) 17.
34. J. Morgós, P. Salley, P. L. Farkas, I. Rusnak, *J. Am. Oil Chem. Soc*., 63(1986) 1209.
35. J. K. Weil, A. J. Stirton , M. V. Nunez-Ponzio , *J Am Oil Soc*., 43(1966) 603.
36. C.D. Drives, R. Clarkson, *J Am Dye Stuff Report*, 20(1931)201.
37. M. Matsuoka, Y.Moroi *Current Opin Coll. Interf. Sci*., 8(2003)227.
38. M.J. Rosen, Surfactant and Interfacial Phenomena," 3rd Edition, John Willey and Sons, New York.2004, p. 63.
39. M.M. Khowdiary, A.A. El-Hanaway, A.M. Shawky, N. A. Negm, *J. Mol. Liq.*, 320 (2020) 114504.
40. M. Abdallah, M. Alfakeer, Mubark Alshareef, H. Hawsawi, Salih S. Al-Junaid, R.S. Abdel Hameed, M. Sobhi, *Int. J. Electrochem. Sci.,*17 (2022) 220949.
41. J. C Bessone. Mayer, K. Tuttner, W. J. lorenz, *Electrochim. Acta,* 28 (1983) 171.
42. M. Sobhi, *Prot. Met. Phys. Chem. Surf*., 50 (2014) 825.
43. M. Sobhi, M. Abdallah, K.S. Khairou, *Monat. fur Chemie* , 143 (2012) 1379.

44. M. Abdallah, Arej S Al-Gorair, A. Fawzy, H. Hawsawi, R. S. Abdel Hameed, *J. Adh. Sci Tech.,* 36(2022)35.
45. O. L. Riggs Jr. and R. M. Hurd, *Corrosion,* 23(8) (1967) 252.
46. K.J. Laider, Chemical Kinetics, Mc Graw Hill Publishing Company Ltd ,1965.
47. Arej S Al-Gorair, M. Abdallah, *Int. J. Electrochem. Sci,* 16 (2021) 210771.
48. M. Abdallah, M. Alfakeer, Arej S Al-Gorair, A. Al Bahir, M. Sobhi, *Int. J. Electrochem. Sci,* 16 (2021) 210622.
49. M. Abdallah, H.M. Altass, B. A. AL Jahdaly, A.S. Fouda, *J. Mol. Liq.*, 216(2016)590-597.
50. M. Abdallah, Basim H. Asghar, I. Zaafarany, A.S. Fouda, *Int. J. Electrochem. Sci.* 7 (2012) 282.
51. M.L. Free, Corros. Sci., 44 (2002)2865.
52. G. Schmitt, Proceedings of the Sixth European Symposium on Corrosion inhibitors (6 SEIC), Ann Univ, Ferrara, N.S. Sez Suppl N. 8 (1985) Separate paper.
53. I. Zaafarany, M. Abdallah, *Int. J. Electrochem. Sci*., 5 (2010) 18-28.